

5-2018

# Scintillator-Based UAV

Austin Mullen
*University of Tennessee, Knoxville*, amullen8@vols.utk.edu

Chris Haseler
*University of Tennessee, Knoxville*, chaseler@vols.utk.edu

Sarah Davis
*University of Tennessee, Knoxville*, sdavi125@vols.utk.edu

Brooke McMurrer
*University of Tennessee, Knoxville*, bmcmurre@vols.utk.edu

Tanner Jefferies
*University of Tennessee, Knoxville*, tjeffri1@vols.utk.edu

***See next page for additional authors***

**Author**
Austin Mullen, Chris Haseler, Sarah Davis, Brooke McMurrer, Tanner Jefferies, and Peyton Lara

# Scintillator-Based UAV

Group Members: Chris Haseler, Sarah Davis, Brooke McMurrer,
Tanner Jeffries, Peyton Lara, Austin Mullen
Mentor: Dr. Hayward
Submitted to: Dr. Miller
NE472 Spring, 2018 Senior Design Final Paper
Date Submitted: May 8, 2018

**The Team**

| | | |
|---|---|---|
|  |  |  |
| Austin Mullen | Brooke McMurrer | Chris Haseler |
|  |  |  |
| Peyton Lara | Sarah Davis | Tanner Jeffries |

**Table of Contents**


1. Objectives
2. Introduction
    2.1. Background Information
        2.1.1. Inputs
        2.1.2. Outputs
    2.2. Constraints
    2.3. Licensing and Regulatory Issues
    2.4. Standards
    2.5. Benefit of Classes
3. Methods
    3.1. Computational Methods
    3.2. Experimental Procedure
        3.2.1. General Flight Procedure
        3.2.2. Electronics Testing Procedure
        3.2.3. UAV Arm Modification Procedure
    3.3. Work Breakdown Structure
    3.4. Gantt Chart
    3.5. PERT Chart
    3.6. Efforts of Each Team Member
        3.6.1. Sarah Davis
        3.6.2. Chris Haseler
        3.6.3. Tanner Jeffries
        3.6.4. Peyton Lara
        3.6.5. Brooke McMurrer
        3.6.6. Austin Mullen
4. Results
    4.1. Scintillator Design
    4.2. Drone Design
    4.3. Electronics Design
        4.3.1. SiPM Readout

4.3.2. Pulse Shaping and Amplification
4.3.3. Peak Detection
4.3.4. Sample and Hold Detection
4.3.5. Power Supply
4.3.6. Microcontroller Integration
4.3.7. Prototyping
4.3.8. Electronics Testing
5. Observations and Conclusions
6. Future Work

Appendix A: MCU Code
Appendix B: References

**List of Figures**

Figure 1. Pulse Processing Chain
Figure 2. Scintillator Processing Chain
Figure 3. EJ-200 Emission Spectrum
Figure 4. Work Breakdown Structure
Figure 5. Original Gantt Chart
Figure 6. Tracking Gantt Example from April
Figure 7. PERT Chart
Figure 8. Scintillator Geometries Tested in Geant4
Figure 9. Completed Stock Drone
Figure 10. Attachment Brackets
Figure 11. Bracket Removal Process
Figure 12. UAV Signal Processing Electronics
Figure 13. Photomultiplier Tube (PMT) [7]
Figure 14. Silicon Photomultiplier [8]
Figure 15. Wideband, Unity-Gain Stable OPAMP
Figure 16. Standard SiPM Output Pulse Shape [9]
Figure 17. Sallen Key Topology [10]
Figure 18. Pulse Shaping
Figure 19. Shaping Amplifier
Figure 20. Simple Peak Hold Circuit
Figure 21. Sample and Hold Wave
Figure 22. Sample and Hold UAV Circuitry
Figure 23. Power Supply Schematic
Figure 24. Soldering IC to Breakout Board
Figure 25. Functionality Test Setup
Figure 26. LF398 Sample Hold Circuit
Figure 27. Breadboarded Components
Figure 28. Chip on Breakout Board
Table 1. EJ-200 Scintillator Properties
Table 2. Circuitry Components for Prototyping

## 1. Objectives

The objectives of this design project center around the design and construction of an Unmanned Aerial Vehicle (UAV) for the purposes of radiation detection. Originally, a finalized UAV, fully integrated with scintillator detectors, was to be the ultimate deliverable for this project. The drone data acquisition system was expected to record pulse height, time, and temperature data while flying inside of a building. This information was to be sent to and stored within a database for real-time or post-hoc analysis. A GUI was planned to display current operating conditions and counts per minute. The scope has since been scaled back to a proof-of-concept scintillating drone, complete with a pulse processing chain suitable for integration onto the drone body. This project was done in collaboration with an electrical engineering graduate design team, tasked with the design and programming of the electronics chain and microcontroller unit (MCU) for the UAV.

This project was divided into various tasks and milestones. First, designs for the modified rotary UAV body, with a focus in environmental protection and payload planning, were developed. Second, a digital silicon photomultiplier (SiPM) and its associated electronics chain were designed and implemented for the conversion, amplification, and interpretation of the scintillator output. Third, a stable and precise adjustable power supply for biasing the SiPM array was designed and implemented with the electronics chain. Finally, a microcontroller processing unit, along with its software, was developed for system control and data recording. The team was also tasked with implementing a temperature feedback control system to stabilize the gain of the SiPM array on-the-fly.

## 2. Introduction

### 2.1 Background Information

The armed forces are developing UAVs able to fit through windows to search denied or dangerous buildings for potential threats. Radiation detectors have been used on UAVs previously as a payload on the UAV. In order to improve the efficiency of such searches, UAV structural materials could be replaced by scintillator materials to increase their detection ability without significantly increasing the payload. The University of Tennessee nuclear engineering, electrical engineering, and computer science departments have a new research grant to aid in this endeavor. The initial material studies suggest that commercially available plastic scintillators are

already strong enough to replace the structural carbon fiber used in UAVs. The task then became to demonstrate that the replacement of structural materials with scintillator plastics was feasible for radiation detection.

Scintillator plastics work by producing visible light when impinged upon by ionizing radiation, such as gamma rays. Silicon photomultipliers can be utilized to detect this light and convert it into a current pulse. This pulse can then be processed into a digital signal using low-noise amplifiers and a custom multichannel analyzer. This creates a useable signal for microcontroller processing. The pulse processing chain described here is shown in Figure 1.

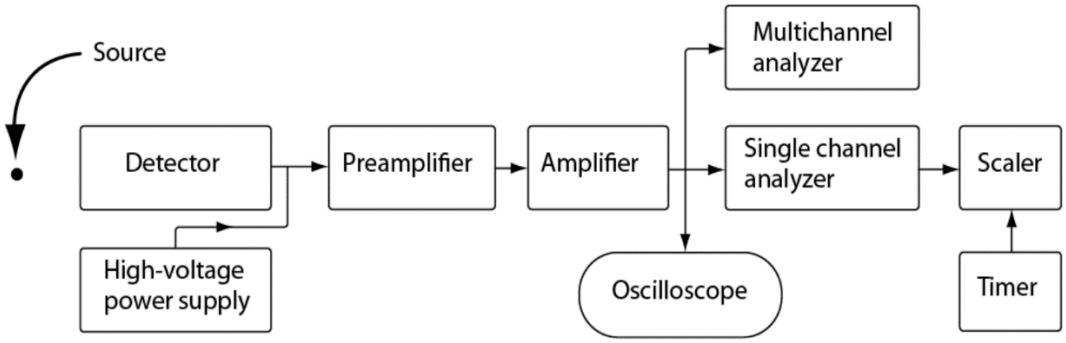


**Figure 1.** Pulse Processing Chain [1]

Figure 2 demonstrates this chain applied to a scintillator detector with a standard readout method.

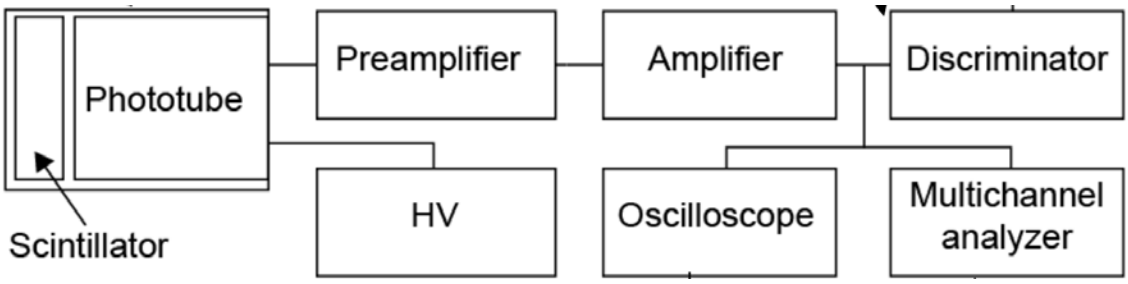


**Figure 2.** Scintillator Processing Chain [1]

The scintillators utilized for this research project were EJ-200 series produced by Eljen Technologies. These scintillators combine two important properties: long optical attenuation length and fast timing. It is the detector of choice for many industrial applications where high sensitivity and signal uniformity are critical operating requirements [2]. These scintillators are

resistant to attacks by aromatic solvents, chlorinated solvents, ketones, solvent bonding cements, and other particles. They were proven to be stable in water, dilute acids and alkalis, lower alcohols, and silicone greases with an understanding that they are safe to use with most epoxies. These properties suited the scintillators well to our purposes in this project. The emission spectrum for these scintillators is portrayed in Figure 3.

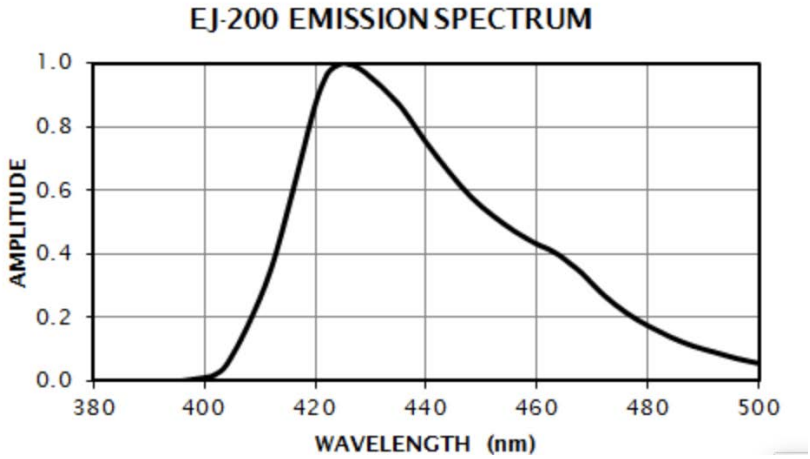


**Figure 3.** EJ-200 Emission Spectrum [2]

Other important properties of the scintillators are given in Table 1.

**Table 1.** EJ-200 Scintillator Properties [2]

| | |
|---|---|
| Light output (% Anthracene) | 64 |
| Scintillation Efficiency (photons/1 Mev e-) | 10,000 |
| Wavelength of Maximum Emission (nm) | 425 |
| Light Attenuation Length (cm) | 380 |
| Rise Time (ns) | 0.9 |
| Decay Time (ns) | 2.1 |
| Pulse Width, FWHM (ns) | 2.5 |
| Refractive Index | 1.58 |
| Softening Point | 75°C |

Organic scintillators consist of aromatic compounds, which are planar molecules made up of benzene rings. Thus, organic scintillators are low-Z materials, consisting of hydrogen, carbon and oxygen, greatly reducing photoelectric efficiency. Although plastic scintillators do not have the greatest resolution or peak efficiency, the objective of this stage of the project is to generate a simple counts-per-minute detector, to demonstrate the proof-of-concept for the design.

It is important to understand, along with scintillation materials and basic electronics chain processing, the various interactions of radiation with matter that determines how detectors process radiation. Heavy charged particles, such as alphas, slow down continuously throughout matter. These particles follow a Bragg Curve, where they travel in a straight path until they have reached a low enough speed that kinetic energy losses are more prevalent. Due the stochastic process of slowing down, these heavy charged particles encounter range straggling, where the total range is different for each initially monoenergetic alpha [3]. This means that two alpha particles of exactly the same characteristics could penetrate slightly different distances into a material.

While heavy charged particles follow a straight path, light charged particles follow an erratic path due to their lower mass, and often experience backscattering. In a backscattering event, a primary electron from the incoming beam is deflected by the electrostatic field of the positive nucleus [4].

Moving on to an understanding of neutral particles, gamma ray interactions are grouped within three main categories: photoelectric effect, Compton scattering, and pair production. The photoelectric effect occurs at low energies, in a process where all of the gamma photon's energy is absorbed by an atomic electron, typically of the K shell of the atom, and takes the form of kinetic energy. The electron then goes on to deposit its energy in the medium as a beta ray. Although the difference between the photon energy and electron binding energy is distributed between the electron and recoil atom, virtually all of the energy is carried as kinetic energy of the photoelectron because of the comparatively small electron mass [5]. As the vacancy left by the photoelectron is filled by an electron from an outer shell, either fluorescence x-rays or Auger electrons may be emitted [5]. This emission is typically approximated to have energy equal to the binding energy of the photoelectron.

With an increase in energy of the incident photon, the next form type of gamma ray interaction occurs: Compton scattering. This photon inelastically scatters with an atomic electron

in the absorbing medium. In this energy exchange, conservation laws apply [6]. In this reaction, only some of the energy from the incident photon is transferred to an atomic electron, resulting in the scattering of both the atomic electron and incident photon.

Finally, once the incident photon energy exceeds the rest mass of two electrons, 511 keV, pair production becomes possible, but not dominant until around 5 MeV. In a pair-production interaction, the incident photon interacts with a nucleus and produces an electron/positron pair. Once the betas slow, the positron annihilates into two 511 keV gammas emitted antiparallel [5]. Pair production is the most effective way to slow down high-energy gammas due to its conversion into two 511 keV gamma pairs regardless of the incident photon energy.

Neutrons are the other uncharged radiation particle of interest. Neutrons deposit their energy in a material through elastic or inelastic scattering, or adsorption. In scattering events, the incident neutron is deflected by the nucleus of an atom, distributing its energy between the itself and the nucleus. In an inelastic scattering event, a gamma ray is emitted from the nucleus to release excitation energy. If the neutron is absorbed by a nucleus, all of its energy is deposited into the medium. However, the resulting nucleus is often in an excited state and may emit a photon that escapes from the volume of interest.

Understanding these types of interactions allowed for the team to predict the physical processes at play within the detection system. With a solid understanding of the previously discussed concepts, the team was able to determine relevant inputs and outputs needed to accomplish the task at hand. This set of inputs and outputs are given below.

### 2.1.1 Inputs

1. Current pulse from the SiPM that corresponds to the energy deposited in the scintillator by some quanta of radiation. The scintillators are made of low-Z constituents, so gamma rays will most likely to deposit energy through Compton scattering within the medium, meaning that the detection efficiency of the system will be low and energy discrimination will be difficult.
2. Temperature sensor for feedback control. The gain of the SiPM is highly dependent on ambient temperature, meaning that pulse-heights will be skewed by changes in the environment. To combat this, a temperature feedback loop would vary the overvoltage on

the SiPM to steady gain, or pulses could be processed post-hoc to adjust their height as needed.

3. GPS capability. The DJI Matrice drone comes equipped with GPS capability. Tagging spectra collected with their locations would be highly valuable to map radiation sources in an area.

### 2.1.2 Outputs

1. Cellular transmission of radiation spectra. Transferring spectra information over a cellular network would allow for real-time data analysis. This would prove highly useful in real-world situations, where the UAV could be used to investigate an area more closely if elevated radiation levels are found.
2. Silicon Photomultiplier feedback control.
    a. Hardware implementation - Feedback from the temperature sensor could be used to vary the overvoltage on the SiPM to steady its gain.
    b. Software implementation - Using a constant overvoltage, pulse heights can be multiplied by a correction factor based on the temperature of the SiPM.
3. GUI display of relevant information. A user-friendly display of spectrum information and other operating conditions would be useful for both testing and real-world applications.
4. Radiation threshold alarms. If the count rate in a certain area exceeds a predetermined value, a radiation alarm should sound from the user control station in order to alert operators.

## 2.2 Constraints

This project is constrained by several important factors brought about by its nature and its scope. The most limiting of these constraints is in size and weight. As the entire detection system has to fit onto a small, operational UAV, the type of equipment available for use is severely limited by the payload of the vehicle. A related constraint is that of power consumption, as the drone is expected to be able to operate for at least fifteen to thirty minutes on one battery charge. The UAV must operate off of a 3.7V battery with 22000mA/Hr capacity and a 7400 mW power limit. Adding larger batteries to provide adequate power rapidly comes into conflict with the size

and weight constraints, so a balance must be struck between the two. From preliminary planning, it was concluded that the drone power would not exceed 4W.

Another major constraint is that of health and safety, as UAV operations can be dangerous if not done carefully. With this constraint, the team faced regulatory hurdles as expected for a project entailing possible danger to others. Steps were taken with industry experts to ensure safety was at the forefront of the UAV operation.

A further constraint is that of ease of modification. The UAV must have removable arms for replacement with scintillator materials. This limits our options drastically as very stable uni-body drones would prove intractable for this purpose. A final constraint is economic, as the components needed for this project, particularly the drone system and SiPMs, were expensive, and funding for this project was limited. The manufacturing costs, including the microcontroller, general sensors, communication units, and system boards, were to not exceed $2000. This constraint required that parts be ordered with cost analysis in mind.

## 2.3 Licensing and Regulatory Issues

The use of a UAV system is inherently risky and is thus subject to intense scrutiny and regulation by the university. Purchasing the UAV required the submission of paperwork and approval from the Office of Risk Management on campus, which was successfully obtained. Once the UAV was purchased, a new set of regulatory obstacles had to be overcome in order to actually use the system. Fortunately, Dr. Matt Cook, who has worked with UAV research on campus, graciously offered to help us through this process and allowed us to fly under his Certificate of Authorization (COA), on the condition that he be present for all test flights. Thanks to this, we were expected to merely be able to obtain approval for test flights by submitting flight plans and procedures seven days before the scheduled operations. As the UAV couldn't be operated on campus, all test flights would have been conducted at the University of Tennessee Arboretum in Oak Ridge, where Dr. Cook conducts his own research. Unfortunately, administrative issues with the COA and pre-flight approval prevented full-scale test flights. To compensate, hover tests were conducted to ensure the drone was continuously operable.

## 2.4 Standards

The most important standards applied to this project was the Federal Aviation Administration's (FAA) standards for flight-worthiness. After major changes to the drone's design or structure, the system had to be proven "flight-worthy" and thus did not pose an undue risk to those around its operations. For the enforcement of the flight proposal, the team utilized the FAA Modernization and Reform Act of 2012 (FMRA). Section 226 of this document supports the educational use of unmanned aircraft systems. In addition to these federal regulations, university standards include FI0405 and FI0605, which relate to fiscal policy. These documents cover Unmanned Aerial System (UAS) coordination, use, control, maintenance, repair, and disposal. With the standards imposed by these documents, the team had to communicate with UTPD and the FAA to ensure adequate modifications were made, focusing first on the safety of those around the drone during operation.

## 2.5 Benefit of Classes

NE 401, Radiological Engineering Laboratory, has contributed a large amount not only to our understanding of radiation detection but also to our understanding of the pulse processing chains required to create usable output from the detector. The knowledge learned from this class was applied to create a smaller version of this electronics chain that can fit onto the UAV body without exceeding payload capacity. Understanding detector efficiency was also vital to the design of the detector arms to ensure maximum signal generation. Concepts from ECE 301, Circuits and Electro Mechanical Concepts, had to be used to understand the basics of the complex electronics chain design. NE 402, Nuclear Engineering Laboratory, has also contributed to our understanding of computational modelling of radiation detection as knowledge of MCNP was obtained from this course. Techniques learned in NE 471 and NE 472 were helpful in successful project management. Finally, ME 321, Mechanics of Materials, has contributed to our understanding of the stresses and strains that will be experienced by the detector arms during flight, which will inform our method to couple the arms to the drone body so that they may withstand any stresses experienced.

## 3. Methods

### 3.1 Computational Methods

Modelling work was completed in Geant4 to determine optimal scintillator geometries and configurations to maximize detector efficiency and light transport. Three scintillator arm geometries, with square, circular, and hexagonal cross sections, were available for use, each with a hollow and solid variation. It was important to choose from these the geometry that outputs the strongest signal per energy deposited. To test this, each geometry, the circular, rectangular, and hexagonal solid cross sections, was modelled in Geant4. The hollow cross section designs were not modeled because they were found to be incompatible with the SiPM geometry utilized for this project. Each geometry was impinged upon by a beam of Cs-137 gamma rays (662 keV), and a detector, modelling the SiPM, was placed at the end of the arm. The number of optical photons reaching this detector was then counted and compared for each geometry. This allowed for a calculation of relative detector efficiencies between each geometry, by comparing the number of optical photons collected by each for the same number of impinging gamma rays. The modelling was limited to determining only relative detector efficiencies, and not absolute efficiencies, because it was determined that the absolute detector efficiencies of each geometry were not useful enough in future design work to justify the effort required to calculate them.

Results from the model showed that the square cross-section arms were most efficient for detection, and thus normalized to 100%, while the circular cross section design was 82% as efficient and the hexagonal cross section design was 70% as efficient. This would suggest that the square cross section would be the best choice for the final geometry design. However, as the payload of the drone was a great concern, the signal-to-weight ratio of each geometry was of interest. To calculate this, the relative efficiencies given above were divided by the volume of the detector arm. Since the arms are all of uniform densities, the volume and weight of the arms are strictly proportional. The circular design was found to have the greatest signal-to-weight ratio, at $8.71\%/in^3$, followed by the square geometry at $8.33\%/in^3$ and the hexagonal geometry at $6.76\%/in^3$. Additionally, the circular design was well suited for integration with the drone body and had favorable aerodynamic properties over the other given geometries. Therefore, the circular design was utilized for this project.

## 3.2 Experimental Procedure

### 3.2.1 General Flight Procedure

The main goal and focus during flight of the UAS was to maintain safe operation and mitigate all possible risks. The team's goals were to safely fly the UAS at an altitude below 400 feet above ground level to gain an understanding of the drone's operation to further support the redesign of the UAV arms. The team planned to fly the drone for as long as the battery allowed around the test facility and, at the completion of the flight, safely land the UAV. Multiple batteries would be utilized and recharged to maximize experimental time. This test flight would allow one to get a better understanding of how outdoor conditions, such as gusts of wind, affect flight. Due to the regulations and COA issues, however, the drone has not been test flown. Instead, the drone has been hover-tested in a laboratory setting to ensure proper functionality. It remains as future work to carry out full test flights after modifications have been completed and licensing issues resolved. Flight of the modified drone will be a true test of the operability and sustainability of the system as a whole.

### 3.2.2 Electronics Testing Procedure

Electrical components were ordered and then soldered to breakout boards, to be used in a breadboard. The electrical systems to be included on the drone were then tested through breadboards without being implemented and tested with the drone itself. This was achieved using a voltage generator and multimeter. The electronic components tested include operational amplifiers, pulse shaping circuitry, and an analog to digital converter, in the form of a peak-hold circuit and MCU. Functionality was verified with test methods specific to each component, including using the voltage generator for input and logic signals.

### 3.2.3 UAV Arm Modification Procedure

The UAV arms on the DJI Matrice 100 were made of carbon fiber. These arms were secured to the drone body and the motors, making disassembly difficult. The team found, once the motors were completely detached and the arms removed from the body, that the brackets were secured to the arms with aircraft-grade silicon. This posed a major issue for the team as the brackets were necessary to implement the scintillator as the arm with the rest of the body. The team attempted to use acetone to remove both the brackets from the carbon fiber arms, but it

proved ineffective. They may be removable by making incisions in the carbon fiber so that silicon can be better exposed to the acetone, or through the use of a heat gun. Failing this, it may be necessary for the brackets to be 3D printed for use on the scintillator arms, with special care taken to maintain structural integrity.

Another aspect of the UAV arm modification was the modification and packaging of the stock EJ-200 scintillators for integration into the UAV. Once the UAV was received, it was discovered that the arms of the UAV were slightly smaller than the 1-inch diameter that was quoted by the manufacturer. The actual diameter of the stock carbon fiber arms was measured to be 0.87 inches. This posed a problem as the EJ-200 scintillators purchased were 1 inch in diameter. These EJ-200 scintillators were also 17 inches long while the length of the UAV arm was 10 inches. Ordering custom scintillators from Eljen with the required 10-inch length and 0.87 inch diameter was considered. However, due to a lengthy lead time required for the manufacture of specific dimensions, this option was ruled out. The team consulted with a local company, Agile Technologies, that has experience lathing scintillators. This was determined to be the best option considering both time and budget constraints. By this time, it was determined that the project had transitioned to a proof of concept. Therefore, it was determined that only one scintillator would be lathed for the purpose of benchtop testing and an attempt at integrating the scintillator with the UAV. The EJ-200 scintillator was lathed to the proper size by Agile Technologies, and then packaged in Teflon and electrical tape. Multiple options were considered for packaging, including titanium dioxide paint and photographic tape. Ultimately, it was determined that Teflon tape and electrical tape would be used to package the scintillator, due to off-the-shelf availability with no lead time and better environmental protection than paint or photographic tape. The scintillator was wrapped in 7 layers of Teflon tape to ensure no light would escape the scintillator and 3 layers of electrical tape to prevent any outside light from entering the scintillator. This scintillator was used for bench top testing for the proof-of-concept electronics chain.

### 3.3 Work Breakdown Structure

A work breakdown structure was developed at the start of the project in an attempt to create manageable tasks and goals from the project's large scope (See Figure 4).

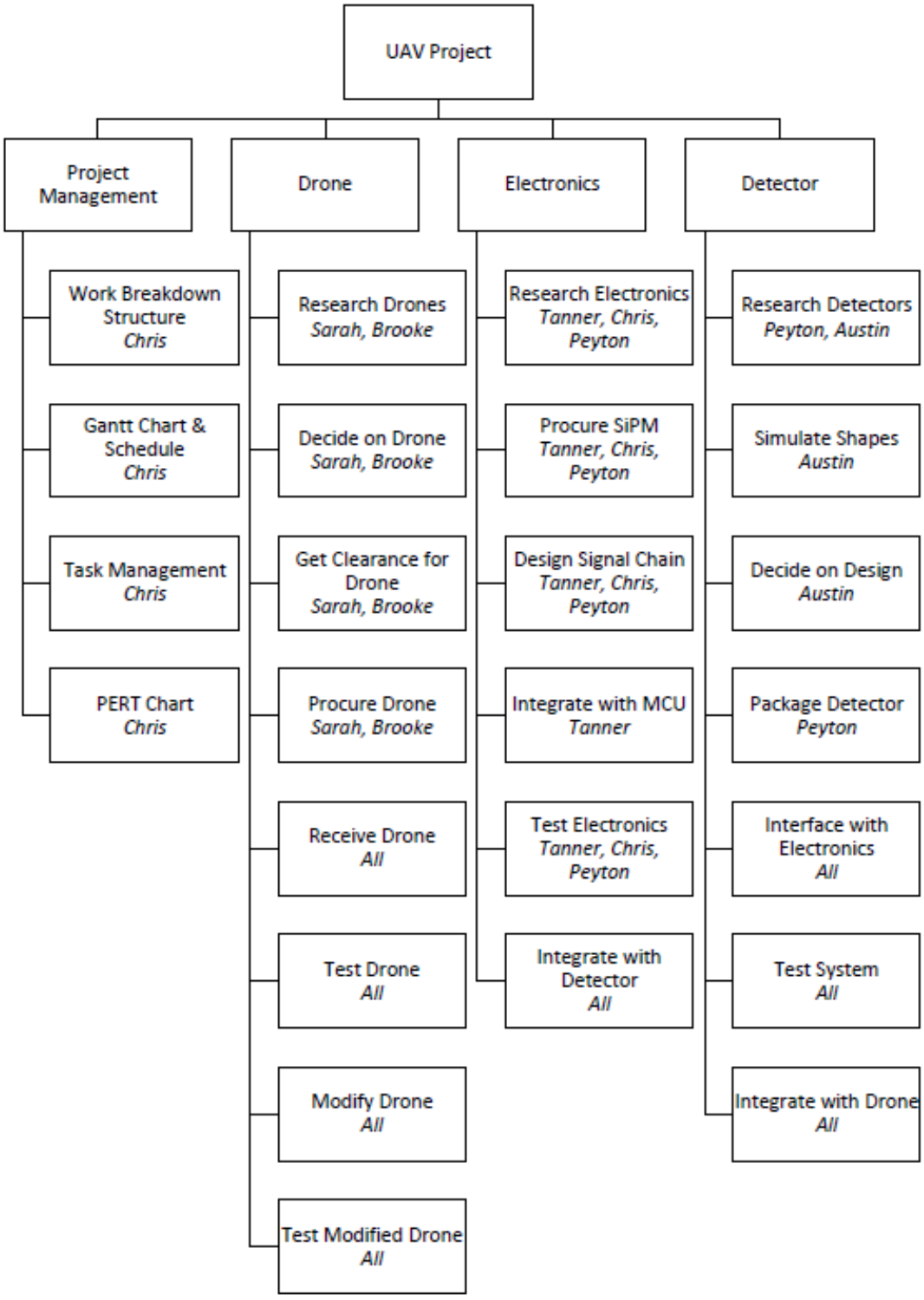


**Figure 4. Work Breakdown Structure**

## 3.4 Gantt Chart

In addition to the Work Breakdown Structure, a Gantt Chart was created using Microsoft Project. This allowed easy scheduling of different aspects of the project, following a similar structure to the WBS (See Figure 5).

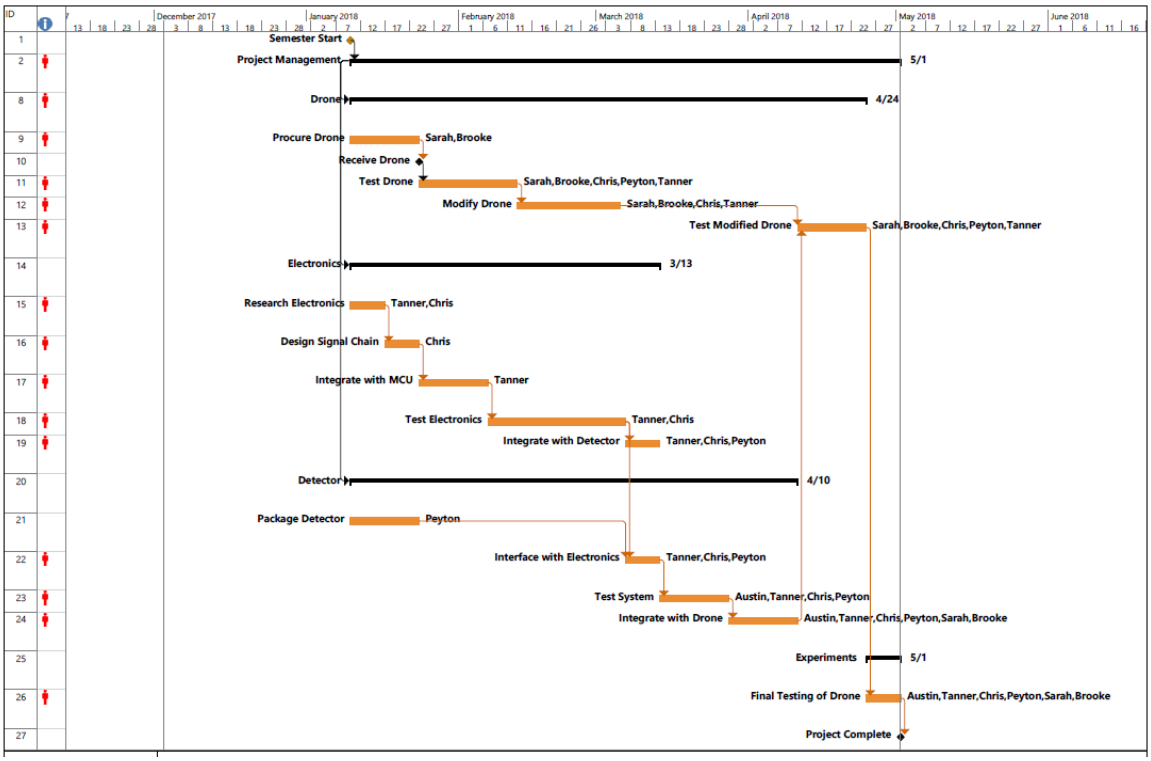


**Figure 5. Original Gantt Chart**

Throughout the project, the Gantt chart and schedule was updated to reflect what tasks had been completed. A tracking Gantt was utilized to determine where the project was falling behind, allowing the team to properly prioritize work (See Figure 6).

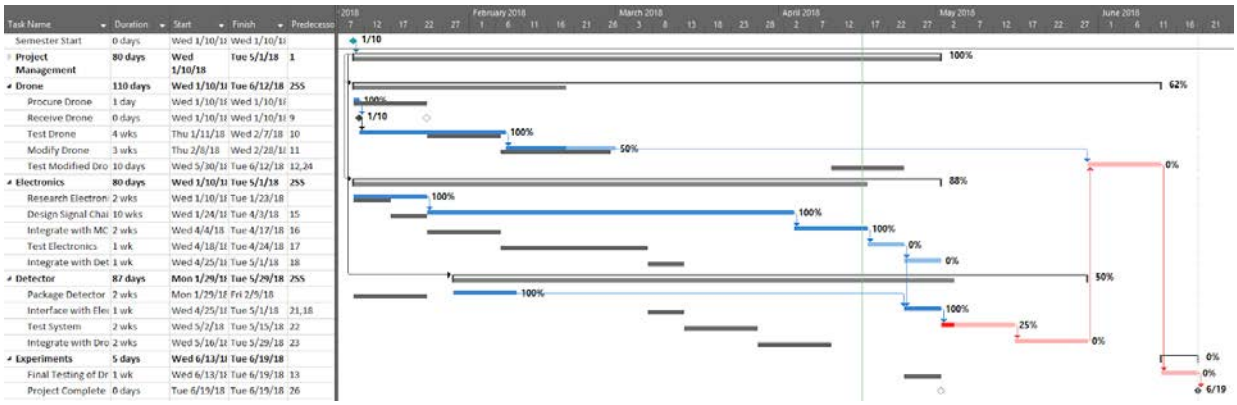


**Figure 6. Tracking Gantt Example from April**

## 3.5 PERT Chart

The Program Evaluation and Review Technique (PERT) chart was also generated using Microsoft Project. This can provide a better graphical representation of task dependencies when compared to a complicated Gantt chart (See Figure 7).


**Figure 7. PERT Chart**

## 3.6 Efforts of Each Team Member

### 3.6.1 Sarah Davis

At the beginning of the project, my main task had been mostly working with the selection of the drone with Brooke McMurrer. There were many aspects of the drone that we needed to consider, with many constraints as well. The main components that we needed to focus on included weight payload, flight duration, size, battery, and arm capabilities. After considering all of these, we decided that the DJI Matrice 100 Drone would be the best fit for our project. The Matrice has a weight payload of 3.6 kg which was significantly higher than everything else we looked at. With this payload, it has a flight duration of over 40 minutes fully charged. The drone also has a dual battery component, which would be very beneficial for us since we would need an extra battery source for the components we will add to the drone. This drone also has removable arms, which is the biggest highlight, since the base of our project is to manipulate the arms with scintillator detectors. The only concern we have would be the size of this drone for indoor use, but in collaboration with the CS and EE teams, we decided it would not be

detrimental. After choosing this drone, we had several meetings with Dr. Matt Cook to make sure we had all the necessary paperwork to move the project and purchasing process forward. With purchasing and testing the drone, there are many precautions taken. We were able to purchase, register, and insure the drone through UTK and FAA. Although we made plans to fly our finished drone with Dr. Matt Cook, the scope of our project changed, so we did not follow through with these plans.

As the project continued, I helped the team with the research of our electronics and signal processing chain. Since we did not originally understand the scope of the work on the electronics chain, the entire second semester was mainly dedicated to figuring it out. I mainly focused on researching the peak hold circuits and the different types of amplifiers necessary to complete our circuits. Finally, I've helped the team present to our senior design course and the Nuclear Engineering Board of Advisors.

### 3.6.2 Chris Haseler

Through the course of this project, I have served as the team leader in addition to the other roles I served on the team. As the team leader, I focused on many of the project management essentials, from the first schedule drafted to the last team meeting held. In this role, I created the Work Breakdown Structure, as well as the Gantt and PERT charts (see Attachments). These original project management tools allowed us to see the overall project goals and break them into smaller, more manageable goals. I created the Gantt and PERT charts using Microsoft Project. I used these throughout the year to track our progress against our original baselined schedule. As can happen with any project, we fell behind schedule during our spring semester, but using Microsoft Project, we were able to see our critical path and where to focus our efforts. In addition to using MS Project, I used a productivity tool called Producteev to delegate and track individual tasks. These tasks ranged from a simple "email vendor" to figuring out how to package the scintillator. The team effectively utilized this tool to prioritize their work. In hindsight, I would have used this tool more often, as it holds team members accountable and sets deadlines for work.

Other than acting as team lead, my primary focus this year was working on the electronics design. As discussed in this paper, the electronics became the most challenging portion of the project, and as the student with the most experience with analog electronics, I led

the charge on our design. I reached out to industry contacts for their advice and developed schematics based on their feedback. Much of the electronics design came from the IC datasheets and suggestions from Dr. Lorenzo Fabris and Jeff Preston. I developed many iterations of the design until both of the contacts were happy with the schematic.

Once the design was done, I worked with Brooke and Callie Goetz to select and order all of the appropriate parts. After the components arrived, I used liquid solder to mount the SMD chips onto breadboardable adapters. When all the parts were soldered, I used a multimeter and voltage generator to test functionality.

### 3.6.3 Tanner Jeffries

During the beginning of the year, my responsibilities rested primarily in communication with the other design teams, primarily the Electrical Engineering design team as they designed the signal processing circuitry. Once they finished their work at the end of last semester, I worked towards implementing their designs in to our own, assisting Chris Haseler with signal processing and power supply chain design. Working with industry professionals, we devoted a lot of our effort to ensuring the design of a working signal processing chain. Even though this proved to be more difficult than we anticipated, the help that we received proved valuable in selecting components that are sufficient in our proof of concept design. Alongside this design aspect, I also helped Peyton Lara with packaging the scintillators, once the appropriate materials for packaging were selected. I also worked in deconstruction of the Matrice platform to assess what modifications needed to be done in order to accommodate the packaged scintillators. Once the scale of the project changed to a proof-of-concept design, we began to focus more on ensuring that our ideas and processes can be interpreted and implemented by future teams.

### 3.6.4 Peyton Lara

Through this year, my main responsibilities have dealt with the scintillator modification and packaging. My main responsibility of scintillator modification arose from the decision to modify the existing EJ-200 scintillators to match the size of the UAV stock arms. This decision was made after I obtained quotes from Eljin for a custom scintillator and from Agile Technologies for scintillator lathing. The scintillator was lathed by Agile, and then polished by myself with the help of Caleb Redding in order to ensure the best performance. After considering

many options including Teflon tape, Titanium Dioxide paint, photographic tape, and electrical tape, we decided based upon the recommendations of both Dr. Hayward and Dr. Fabris at ORNL and cost effectiveness, we decided to use Teflon tape and electrical tape to package our scintillators. The Teflon tape was wrapped around the modified scintillator to ensure efficient light transport through the scintillator to the SiPM. The electrical tape was wrapped over the Teflon tape to ensure a light tight packaging was created. This setup was used for our lab testing of the electronics chain. I was able to help integrate the scintillator and SiPM into the electronics chain for proof of concept in our electronics chain. We predict that we will need an extra outer layer of packaging in order to better protect our scintillator from the environment once it is integrated into the UAV. A likely candidate for this outer packaging is heat shrink wrap. However, this was not necessary to implement as the scope of the project changed to a proof of concept.

### 3.6.5 Brooke McMurrer

This year, my main tasks have resided in all efforts regarding the UAV selection and alteration as well as circuitry development and part procurement. Through the desire to obtain a drone capable of sustaining a large weight payload, Sarah and I explored the available drone options fitting our weight and size constraints. Through our analysis, it was determined that the DJI Matrice 100 drone was a good fit for our UAV project for multiple reasons. First, it had a hefty payload of 3.6 kg, which was higher than most other drones that had payloads of less than 1 kg. Second, it possessed a dual battery compartment on the base of the Matrice. The current incorporated battery had a voltage output of 22.8 V, making it fully functional for our needs. Third, the Matrice 100 had removable arms, which allowed our team to attempt manipulation of the arms by attaching the scintillators and their respective components, without having to break apart the drone. After this determination was made and the purchase request was enforced, Sarah and I conducted multiple meetings with Dr. Matt Cook to determine the process moving forward to ensure our drone was insured. We took on the tasks of getting our drone insured and registered through UTK and the FAA. In our effort to succeed, we attended a flight test at ORNL to learn the appropriate flight procedures. After gaining this experience, Sarah and I produced a white paper to ensure our flight procedures were adequate, moving forward, allowing us to fly under Dr. Cook’s COA in the near future.

Moving into the second semester of our project, our team faced the issue of brackets being strongly adhered to the carbon fiber arms. These brackets are necessary for implementation of the scintillator materials. Austin and I worked diligently with acetone to remove the brackets, but failed. Due to our decision to finish this years work in the prototyping phase, the removal of the brackets will not be completed this year, but will be revisited in the coming semesters. Finally, I supported electrical component procurement by meeting with Dr. Callie Goetz, formulating part lists and purchasing needs to complete the circuitry in a timely manner.

3.6.6 Austin Mullen

I have primarily performed programming duties for this project, as I have the strongest background in software development. First, I created a model of the drone system in Geant4 to test the optical transport properties of different scintillator geometries. I had never used Geant4 before, and the tool came with a steep learning curve, but with the help of Micah Folsom I was able to finally develop a working optical transport model for the scintillator. I was also tasked with being the main point of contact with the computer science design team working to develop a navigational program for the drone. However, as the project developed, our two teams' goals diverged and close collaboration was no longer necessary. I also helped to understand the pulse processing electronics chain needed to convert the output from the SiPM to a digital signal useable by the microcontroller.

This task continued into the second semester of work on this project. As the electronics chain began to take shape, I focused primarily on the MCU integration to the circuit and helped with the power supply development. To meet those goals, I developed code for the Teensy MCU we utilized for the project and ensured that it could be integrated with the pulse processing chain without problems. I also aided in the search for chips, such as voltage inverters and voltage step-down chips, that were necessary for the power supply. Finally, I helped in the assembly and testing of the entire electronics system.

## 4. Results

4.1 Scintillator Design

Through the work of this year's design team, we achieved multiple results and found new issues that will need to be overcome in the coming semesters to deliver a completed UAV

system. The Geant4 code provided results regarding the different detector geometries (See Figure 8). It showed that the square cross-sectional design was most efficient for light transport and collection. The circular design trailed behind at 82% relative efficiency and the hexagonal design at 70% relative efficiency. However, because the circular design had the highest signal-to-weight ratio (8.71%/in$^3$ versus 8.33%/in$^3$ for the square and 6.76%/in$^3$ for the hexagonal design), and was most suitable for integration to the drone body without major modifications, it was chosen for the final scintillator design. This final scintillator design was then modified to fit the size of the carbon fiber drone arm by lathing the scintillator from 1” diameter and 17” length to 0.87” diameter and 10” in length. This scintillator was packaged with Teflon and electrical tape and ready for integration with the drone pending the removal of the stock drone arm brackets.

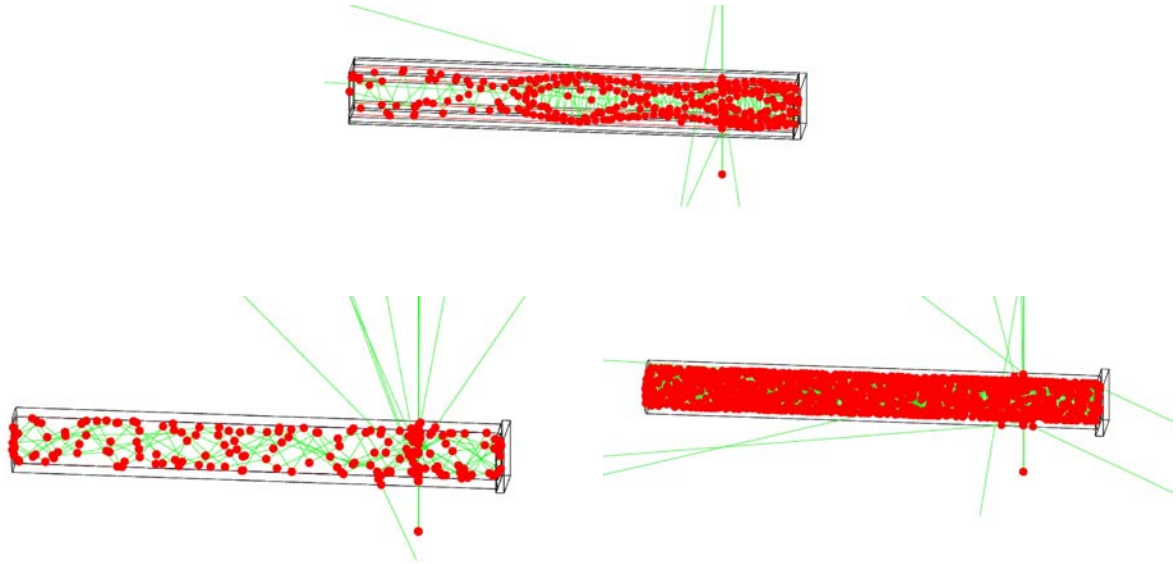

**Figure 8.** Scintillator Geometries Tested in Geant4

4.2 Drone Design

Another accomplishment our team achieved in the first semester was the selection of the DJI Matrice 100 drone. There was much discussion regarding the use of the Parrot Bebop 2, a drone currently owned by the university. After multiple analyses and meetings, it was determined that the DJI Matrice would produce the best results in an attempt to satisfy all project objectives. First, it had a payload of 3.6 kg, which was higher than most other drones of comparable size. Second, there was a dual battery compartment on the base of the Matrice. The current incorporated battery had a voltage output of 22.8 V. With the addition of a second

battery, the power requirements of the UAV would be easily met. Fully charged, these batteries could power the drone to fly for 40 minutes with a maximum speed of 22 m/s, which was sufficient for operations. Third, the Matrice 100 had removable arms. This was expected to allow us to modify the drone without physically breaking apart the drone. The only possible issue with this drone was that the operating temperature was from 10°C to 40°C. This may be a problem if the drone is needed for future use in the Middle East, but we proceeded with the understanding that this would not hinder our usage in Knoxville, TN. Our fully constructed stock drone is shown in Figure 9 below.

**Figure 9.** Completed Stock Drone

After obtaining the Matrice, we encountered multiple issues in attaching the scintillator arms. Brackets were tightly adhered to the carbon fiber arms, portrayed in Figure 10. These brackets are necessary for implementation of the scintillator materials, and therefore need to be removed from the current arms before modifications can take place. Our team attempted to remove the brackets with acetone, a process depicted in Figure 11, but were unsuccessful. Due to the change of scope of this project, the removal of the brackets has been reserved for future design teams.

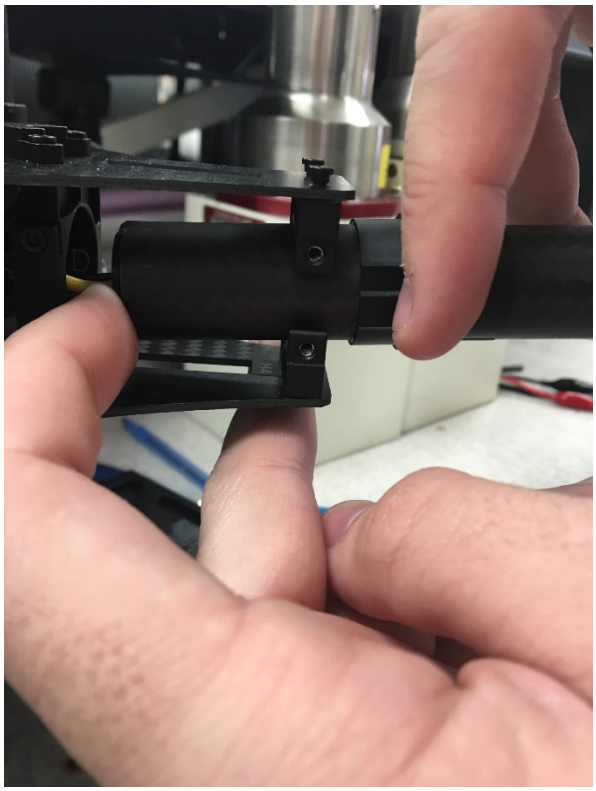

**Figure 10.** Attachment Brackets

**Figure 11.** Bracket Removal Process

Although we were not able to remove the brackets for the implementation on the scintillator materials, we were able to produce scintillator arms ready for attachment. The team utilized Agile Technologies to lathe the scintillator materials down to the appropriate diameter, 0.87 inches from 1 inch, for integration with the drone body. The full arm length required was 10 inches. The arms were also properly packaged to ensure efficient light transport and environmental protection, using both electrical tape and teflon tape. This protected the sensitive scintillator material from the environment and from light-leakage.

After the drone was constructed, the team expected to take the drone for a test flight at the ORNL testing facility. However, due to the regulatory constraints imposed, the team was only able to conduct a hover test with the stock drone. Through this hover test, the team gained an understanding of the DJI software. The DJI Flight Application would allow us to conduct calibration and balance tests on our drone, which would be required once structural modification was complete. The flight test proved the operability of the drone and validated that it was manufactured correctly and was ready for modification.

## 4.3 Electronics Design

The electronics chains for both the power supply and pulse processing of this system had to be constructed from the ground-up, as standard detector electronics are much too heavy and require very high voltages in order to operate. The signal processing chain full schematic is shown below (See Figure 12). Each part of the electronics chain was redesigned as described in this section.

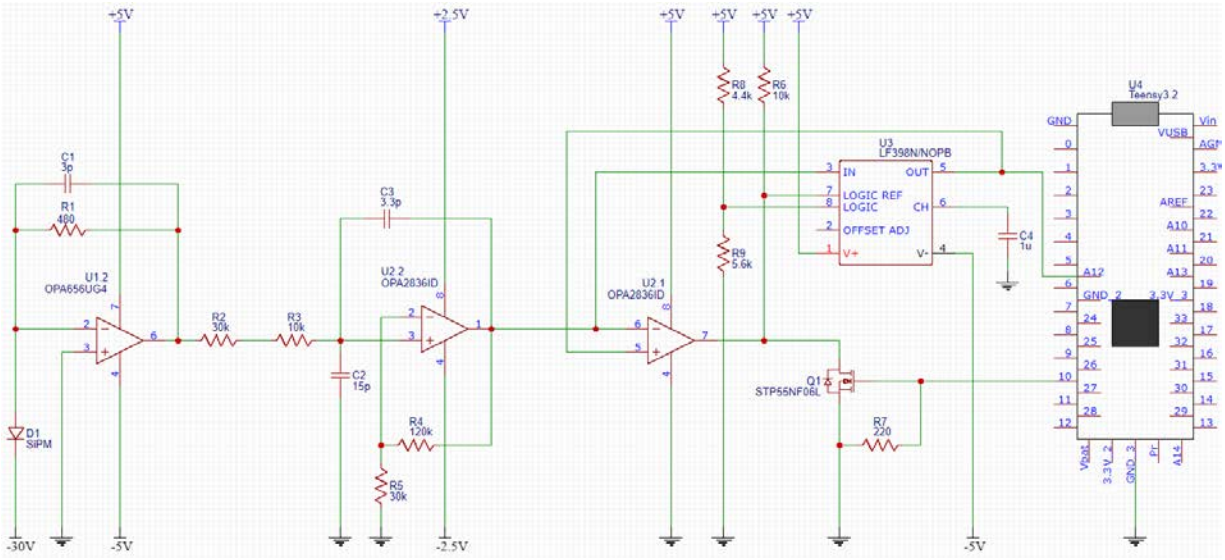


**Figure 12. UAV Signal Processing Electronics**

### 4.3.1 SiPM Readout

In a typical scintillator readout chain, a photomultiplier tube is used to increase the light output from the scintillator into a useable pulse. However, photomultiplier tubes (PMTs) use a high voltage source often in excess of 1000 volts. Due to the power constraints of the drone, achieving this high voltage with sufficient current is nearly impossible. Additionally, PMTs are bulky, heavy devices that take up a lot of space and payload (See Figure 13). It may be possible to mount a single PMT on a drone, but it is not feasible to mount one for each of the four scintillators. Fortunately, an alternative to the common PMT is available in the novel Silicon Photomultipliers.


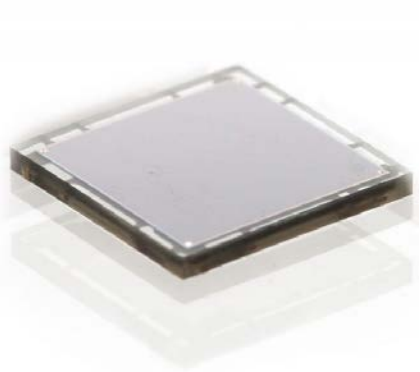

**Figure 13. Photomultiplier Tube (PMT) [7]** **Figure 14. Silicon Photomultiplier [8]**

Silicon Photomultipliers (SiPMs) are sensors designed to combat the disadvantages of PMTs, offering similar capabilities but requiring only low voltages, small size, and physical durability (See Figure 14). SiPMs work by taking advantage of hundreds of silicon 'microcells', consisting of a dense array of silicon photodiodes. In each of these silicon photodiodes, a photon will transfer energy to a bound electron. When these are placed in a sufficient electric field, the silicon will breakdown and become conductive, amplifying the signal in a process termed Geiger discharge. Using many of these microcells in a single SiPM chip results in a signal output proportional to the energy deposited in the scintillator [9].

The SiPM used in this design is a SensL ArrayJ 2x2 SiPM. The chip is incredible small, measuring less than a cubic inch, compared to the massive volume and weight of a PMT. The model selected has four separate SiPM wafers, each with hundreds of microcells. Each of the outputs can be read independently, but they are summed together in this design to maximize the surface area of the scintillator that is read. When adhered to the packaged scintillator, the SiPM outputs a current pulse that corresponds to the radiation energy.

### 4.3.2 Pulse Shaping and Amplification

The SiPM outputs a current pulse when radiation interacts with the scintillator, but the current pulse must be converted, shaped, and amplified before it can be read with digital electronics. In a laboratory environment, this shaping is best done using a NIM "Nuclear Instrument Module" setup. A NIM rack is a standard used in the nuclear industry for instrumentation, and different modules such as an HV power supply and a shaping amplifier can

be directly inserted as needed. Unfortunately, each individual module is larger than the drone itself, so this is not a feasible method. In place of the standard, multi-use NIM modules, each step was custom built with this specific purpose in mind.

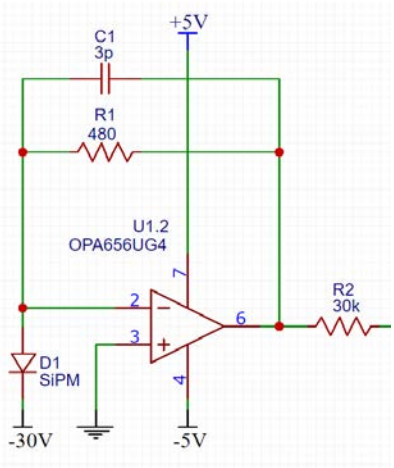


**Figure 15. Wideband, Unity-Gain Stable OPAMP**

The first stage of signal post-processing is to convert the current pulse from the SiPM into a voltage pulse that can be more easily read by digital electronics. This is accomplished using an OPA656 Wideband, Unity Gain Stable, FET Input Operational Amplifier (See Figure 15). Used in conjunction with a capacitor, two resistors, and a +/- 5V power supply, this will convert the current pulse into a fast rise, slow decay voltage pulse (See Figure 16). As the name of the op-amp implies, however, it is a unity gain chip, meaning the magnitude of the signal is not increased at all.

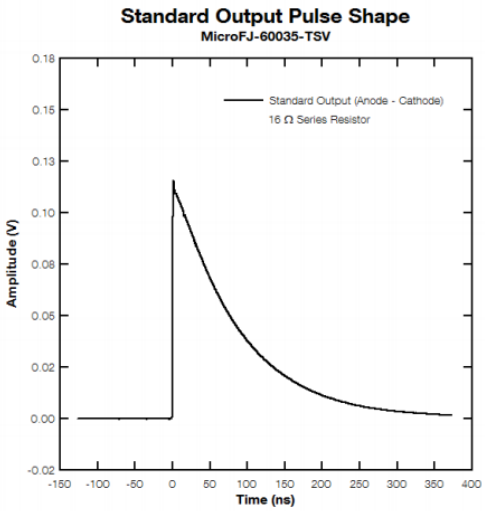


**Figure 16. Standard SiPM Output Pulse Shape [9]**

Once the pulse has been converted into the sharp peak shown above, it is necessary to shape it to a more gaussian-like pulse and amplify it so that it can be read with more precision. Again, however, power constraints make typical shaping methods out of the question. Normally, shaping is done with a series of RC-CR circuits that act as low and high pass filters, with isolating op-amps separating components of the circuit. Using multiple op-amps in this stage is impractical because each can have fairly significant power requirements, and one op-amp is already used to convert the current pulse. In an effort to minimize these power requirements, a single OPA836 Very Low Power, Rail to Rail, Negative Rail In, Voltage Feedback operational amplifier does the heavy lifting in this step.

In order to generate similar results as multiple shaping stages with just one op-amp, a Sallen-Key topology with resistors and capacitors was used (See Figure 17). A shaping time of 1 microsecond allowed second order shaping from the single, low power device. In addition to changing the pulse to a more gaussian-like shape, resistors R4 and R5 have a 4 to 1 ratio, resulting in a 5x voltage gain. This five times gain is more than enough to increase the signal to a desired level, but doesn't run the risk of overpowering the +/- 2.5 volt rails for the low power op-amp. The output from this stage of the circuit is a sufficiently large, properly timed, gaussian pulse (Curve A2 shaped into curve C2 in Figure 18).

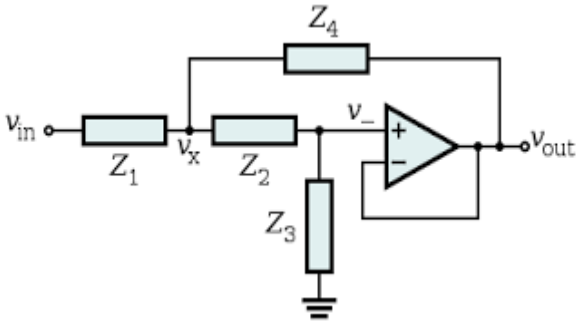


**Figure 17. Sallen Key Topology [10]**

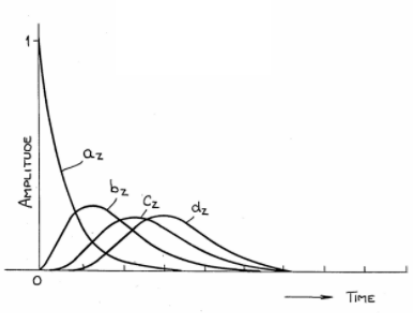


**Figure 18. Pulse Shaping [11]**

The following Figure 19 depicts the amplifier schematic used for the UAV design.

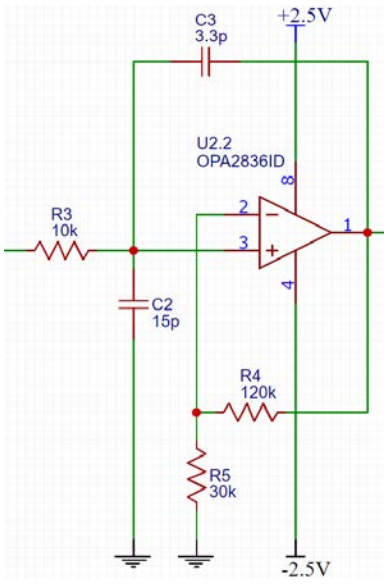


**Figure 19. Shaping Amplifier**

4.3.3 Peak Detection

Accurate peak detection is vital to an effective radiation detection system. Typically, this is accomplished using a multi-channel analyzer, or MCA. A MCA converts an analog peak into a digital signal by using a series of capacitors that charge as the voltage rises. Once the voltage stops rising, a digital signal representing the maximum height of the peak is produced. This allows signals to be converted very quickly, avoiding dead time in the detection system. This system is very effective for most detection scenarios, but is unfortunately unsuitable for use in this project. First, a MCA is very large and bulky, making it impossible to integrate to a drone with stringent size and weight constraints. Second, MCA's must typically be connected directly to a PC with proper software to interpret the signals generated. It would be impossible to run this software on the MCU used with the UAV system, precluding it from use here.

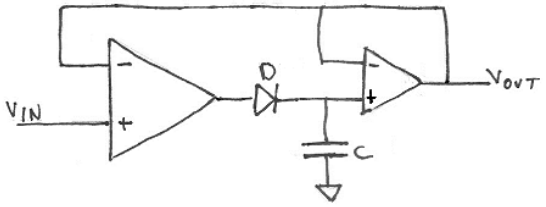


**Figure 20. Simple Peak Hold Circuit [12]**

The MCU is unfortunately much too slow in its processing to directly read in the analog signals produced by the pulse shaping circuit. Because of this, the peak must be prolonged for long enough for the processor to register it as a peak and record its value. This was originally to be accomplished using a simple peak-hold circuit. An incoming peak first begins to charge a capacitor up to its max voltage. Once the peak voltage is reached, the incoming voltage begins to drop but the capacitor is unable to discharge due to a diode. The capacitor thus holds at the peak voltage, prolonging it long enough to be read by the MCU. Once the value was recorded, a digital signal could be produced by the MCU to reset the circuit and drain the capacitor back down to ground.

#### 4.3.4 Sample and Hold Detection

The simple diode and capacitor peak-hold design described above will work well in a laboratory environment, but less so in this application. The circuit has some major drawbacks, namely with the difficulty in effectively resetting the hold in a timely manner and with noise in the signal. The concept for a peak hold circuit would work well in this design, but a more complex circuit with better features is desired.

A sample and hold circuit was more effective than a simple peak hold circuit for the purposes of this project. In a peak hold circuit, an operational amplifier is used as a comparator, along with a LF398 Monolithic Sample and Hold Circuit chip. The LF398 produces an output by either sampling an analog input or holding a previous input voltage. The chip decides whether to sample or hold based on a logic signal that it receives. If the logic input is higher than the reference logic input, the chip samples. If not, it holds its current voltage output. For the circuit used here, the reference logic is provided by the comparator while the logic input is held constant at 2.6 volts. While the comparator shows the input voltage is higher than the output voltage, and thus a peak is rising, the reference voltage is held at 0 volts and the chip samples. Once the output voltage becomes higher than the input voltage, indicating the top of a peak, the reference logic voltage increases to 5 volts and the chip holds. This process is depicted in Figure 21. The peak voltage is held long enough for the MCU to read the peak value and give a logic signal. This signal triggers a MOSFET, which allows the output from the comparator to drain to ground and the LF398 to begin sampling once again, awaiting the next peak.

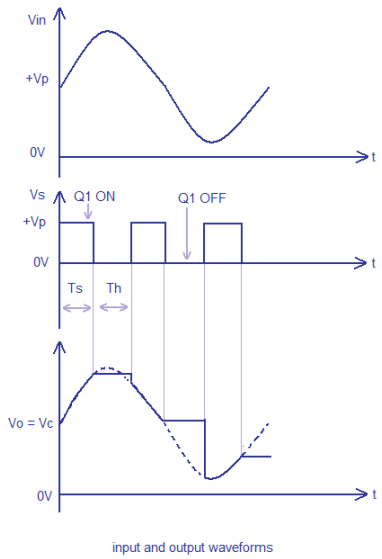


**Figure 21. Sample and Hold Wave [13]**

This part of the circuit is shown close-up in Figure 22.

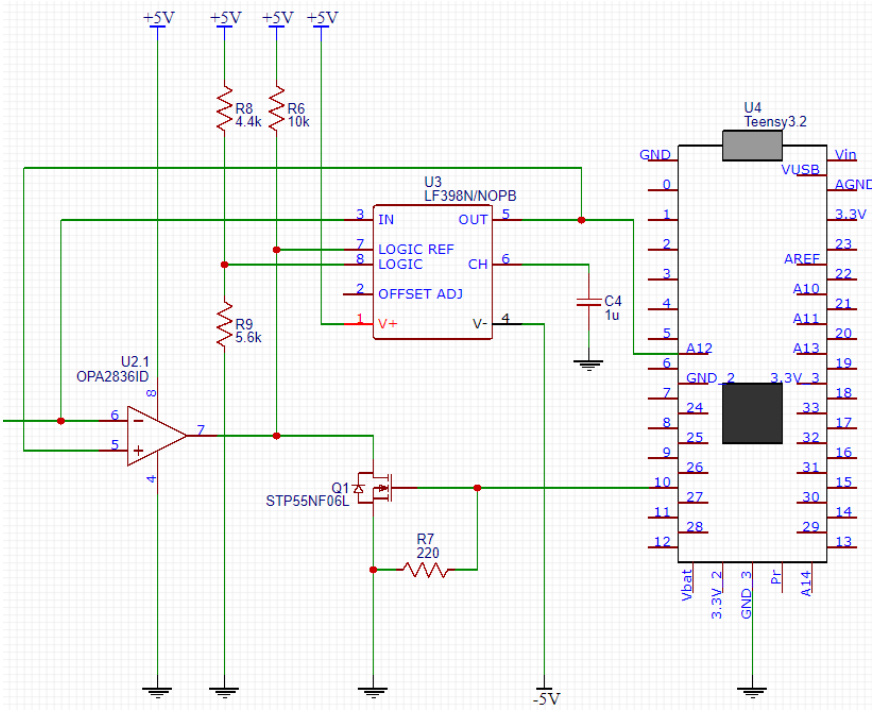


**Figure 22. Sample and Hold UAV Circuitry**

## 4.3.5 Power Supply

The components of the peak-shaping circuit required several different voltages to operate, which must all be provided by a single 3.7 volt battery. To do this, a separate power supply

circuit was devised to provide a positive and negative 5 volts, a positive and negative 2.5 volts, and a negative 30 volts. The smaller voltages were used to bias the operational amplifiers and other chips of the circuit, while the large, negative voltage was used to bias the SiPM.

The entire power supply circuit is shown in Figure 15. The circuit begins with the 3.7 volt Lithium ion battery equipped standard with the drone. From there, a TPS65133 Split-Rail Converter Dual Output Power Supply is used to step the voltage up into a positive and negative 5 volts. The negative 5 volts is then stepped-down by a LM137H883 3-Terminal Adjustable Negative Regulator to a negative 2.5 volts. The positive 5 volts is also stepped-down, this time by a TLV70025 200-mA Low-IQ Low-Dropout Regulator, to a positive 2.5 volts. The positive 5 volts is also stepped-up using a U3V50AHV Adjustable 9-30V Step-Up Voltage Regulator to a positive 30 volts. This positive 30 volts is then inverted using a LTC3261 High Voltage, Low Quiescent Current Inverting Charge Pump to a negative 30 volts.

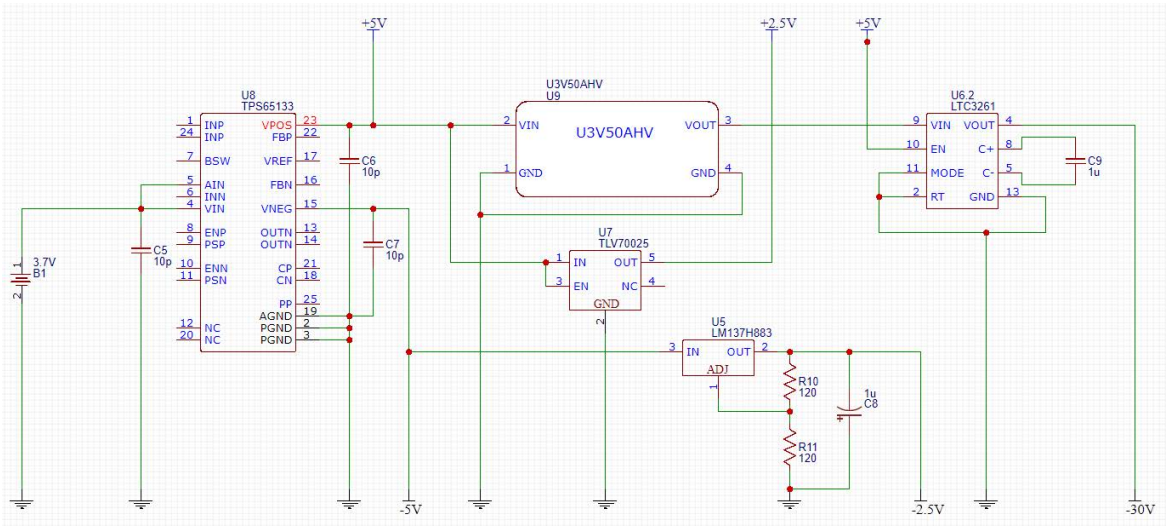


**Figure 23. Power Supply Schematic**

4.3.6 Microcontroller Integration

A Teensy Microcontroller Unit was utilized to record the pulses generated by the detector, along with other relevant information, and to reset the peak-hold circuit in preparation for the next pulse. The code used by this MCU is provided in Attachment 4. The program looped for 15 seconds, during which time it waited for the output from the peak-hold circuit to rise above a threshold value, indicating a peak. It then recorded 5 voltage measurements and averaged them together. This helped to mitigate slight variations in the held peak voltage and any effects of the rise time that may have been seen by the MCU. Because the pulse rose much

faster than the MCU could measure, this was not likely to pose any serious problems. Since the SiPM gain was sensitive to temperature, the temperature at the time of measurement was also recorded. This data could be used to correct the peak heights post-hoc to account for temperature gain effects. Finally, the data entry was tagged with the time of measurement for later identification. While the code presented here does not record GPS locations with the data, this feature would be trivial to include within the existing framework. This data entry was then saved to a string in the computer's internal memory before the reset logic signal is sent to the peak-hold circuit.

After the fifteen second loop had completed, a text file was opened on the computer's SD card, on which all data was to be written. The string was then written to the data file and the file was closed. The MCU then resumed its fifteen second measuring loop. The data was recorded to the SD card in bulk because writing to a memory card is slow compared to recording data in internal memory. Therefore, if data were recorded to the card in real-time, a great loss in recording efficiency would result. The SD card could be removed at the end of testing and inserted into any PC for data analysis.

### 4.3.7 Prototyping

Breadboarding was the most substantial method for testing these electronics chains. In order to construct these circuits, breakout boards were required for various components. The circuitry shown in Figure 9 and Figure 10 includes resistors, inductors, capacitors, Op-Amps, various power supplies, and a Mosfet. Table 1 displays parts required for this circuitry.

**Table 2. Circuitry Components for Prototyping**

| |
|---|
| Resistors (ohm)<br>30, 120, 220, 400, 450, 4k, 10k, 18k, 30k, 120k |
| Capacitors (Farad)<br>3p, 3.3p, 15p, 10n, 1u, 10u |
| Inductors (Henry)<br>4.7u |
| Operational Amplifiers and SH Chip<br>OPA656, OPA2836, LF398 |
| MOSFET<br>STP55NF06L |
| Power Supply |

| |
|---|
| LM137, LTC3261, Pololu U3V50AHV, TLV70025Q |
| Breakout Boards<br>Narrow SOIC-8 to DIP, Breakout for OPA656, SOIC 14 to DIP, 16-Pin LF398 Breakout, TSSOP to DIP for LTC3261, SOT-23 to DIP, WSOON TPS65133 |
| Breadboarding Supplies<br>Board, Wire, Battery, Battery Babysitter, JST Connector, Jumper Wire |

All components described in Table 2 were bought in small bulk supply. To ensure broken components did not halt testing, 3 or 4 times the necessary amount of most components were ordered.

### 4.3.8 Electronics Testing

Once the parts above were received, liquid solder was used to mount the parts on breakout boards with header pins. The solder was applied onto each breakout board with a syringe and the IC mounted on top. Once the chip was in place, a heat gun was used at 250 degrees C to melt the solder, secure the chip to the board, and ensure a good electrical connection. After the chip was soldered to the breakout board, header pins were attached in a similar manner. This process was repeated for all the ICs. This allowed the chips to be easily mounted into a breadboard in a manner that allowed troubleshooting and testing.

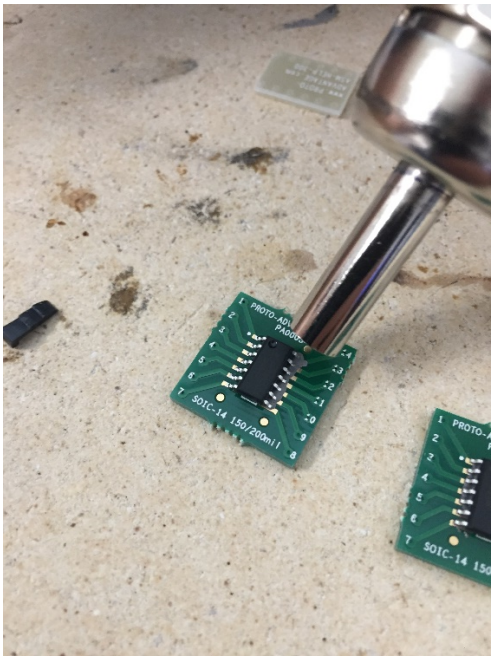

**Figure 24. Soldering IC to Breakout Board**

With the parts in the breadboard, basic functionality testing was conducted. Using a voltage generator, the comparator chip was tested first. This chip successfully output the proper logic signal according to the design and input signals. The actual output values were not exactly 0 and 5 volts as initially expected, but were within a 1-volt tolerance that is compatible with the LF398 sample and hold chip.

After testing was completed on the comparator, the sample and hold chip was tested for functionality. Again, this was tested using a voltage generator which provided test and logic signals. The sample and hold chip worked as expected. Additionally, power supply components were tested individually and each worked as designed. Further testing for the signal chain was desired and is still necessary but was not completed due to time constraints.

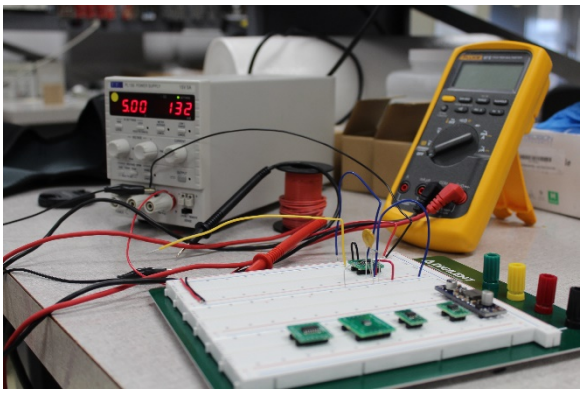

**Figure 25. Functionality Test Setup**

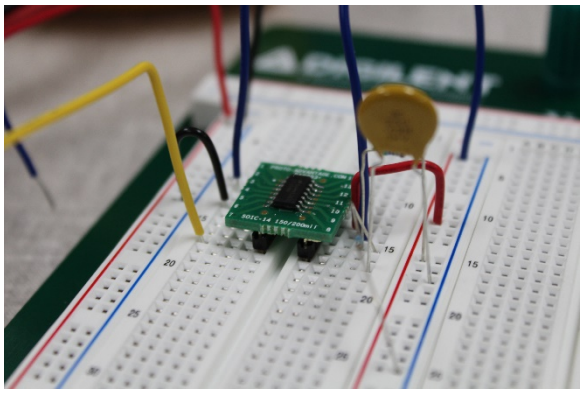

**Figure 26. LF398 Sample Hold Circuit**

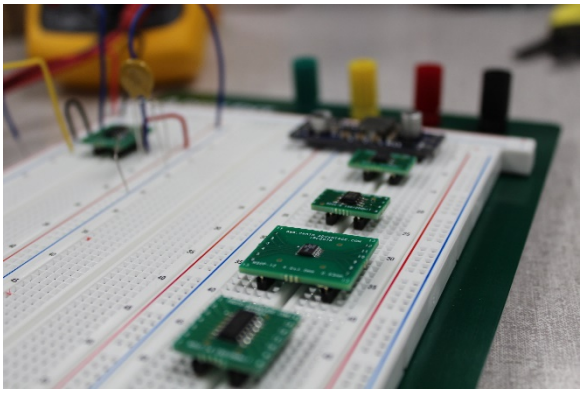

**Figure 27. Breadboarded Components**

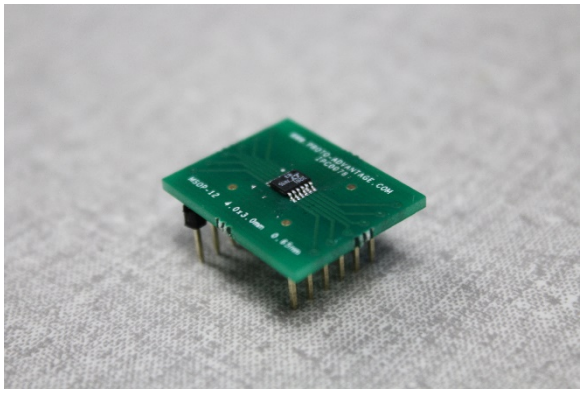

**Figure 28. Chip on Breakout Board**

## 5. Observations and Conclusions

There have been many important conclusions drawn from the work on this project over the last two semesters. First, and most importantly, it was concluded that replacing UAV

structural materials with scintillator detectors for the purposes of in-flight radiation detection with minimal payload restrictions is feasible. The benchtop, proof-of-concept tests carried out during this semester have proven this feasibility. A second conclusion reached during the work of this semester was that the miniaturization of pulse-shaping electronics is far from a trivial task, and requires thorough thought and even some trial-and-error experimentation to function. A final conclusion reached was that modifications to pre-existing and packaged hardware, such as the drone body, are often difficult, highlighting the importance of researching the ease-of-modification of components before purchasing.

## 6. Future Work

Due to the reduced scope of this project due to time and licensing restraints, there remains further work to be done in an attempt to achieve a fully functional drone. Primarily, a proof-of-concept scintillator arm developed with the design from this semester must be integrated with the drone body. This process begins with fully implementing all of the required components for the platform's environmental feedback, such as the GPS module and temperature sensor. Seeing as though the temperature feedback capacity is currently programmed into the MCU, all that would be necessary for this aspect would be to select and test a temperature probe that would be precise enough for the needs of the SiPM. As far as the GPS module is concerned, the DJI Matrice platform by default includes a module that provides GPS feedback, so all that would need to be done in this regard is transmit the data to the MCU, where it can be processed and used to assist in drone control. Once this is complete, and all of the modules are tested and shown to perform their desired function, the drone can be recalibrated for flight, taking into account the added weight from the new components. After this, the licensing issues can be addressed and resolved and the drone can be taken for a full-scale test flight.

## Appendix A: MCU Code

```
/*
  DATALOG_UAV V0.2

  Program to log data from both the temperature sensor and the SiPM outputs onto a SD card.
  Created by Austin Mullen on 2/18/18
  Based on the DataloggerTEENSY3.5 code created byt Tom Igoe

*/

#include <SD.h>
#include <SPI.h>

const int chipSelect = BUILTIN_SDCARD;

//Set pins for data input/output:
//MAKE SURE TO CHANGE THESE TO MATCH PHYSICAL DESCRIPTION
#define tempPin 0
#define detPin1 1
#define detPin2 2
#define detPin3 3
#define detPin4 4
#define outputPin 5

void setup() {

  pinMode(tempPin, INPUT);
  pinMode(detPin1, INPUT);
  pinMode(detPin2, INPUT);
  pinMode(detPin3, INPUT);
  pinMode(detPin4, INPUT);
  pinMode(outputPin, OUTPUT);

  //Open a serial communication and wait for the port to open
  Serial.begin(9600);
    while (!Serial) {
      ;
    }

  Serial.print("Initializing SD card...");
  if (!SD.begin(chipSelect)) {
    Serial.println("Card failed or not present");
    return;
  }
```

```
  Serial.println("Card initialized.");

}

void loop() {

  //Set a threshold value for recording detector measurement
  //We will likely need to trial-and-error our way into finding this
  float detThreshold = 0.1;
  int t = millis(); //Time
  int told = millis(); //Old Time
  // Make a string to collect the data
  String dataStr = "";
  // For 15 seconds...
  while (t-told<1500) {
    // Check and see if the detector response is over the threshold value
    float detSensor11 = analogRead(detPin1);
    float detSensor21 = analogRead(detPin2);
    float detSensor31 = analogRead(detPin3);
    float detSensor41 = analogRead(detPin4);
    if (detSensor11 > detThreshold || detSensor21 > detThreshold || detSensor31 > detThreshold
|| detSensor41 > detThreshold) {
      // Read the sensors and add it to the data string
      float tempSensor = analogRead(tempPin);
      //Repeat this process 5 times to obtain an average
      float detSensor12 = analogRead(detPin1);
      float detSensor22 = analogRead(detPin2);
      float detSensor32 = analogRead(detPin3);
      float detSensor42 = analogRead(detPin4);

      float detSensor13 = analogRead(detPin1);
      float detSensor23 = analogRead(detPin2);
      float detSensor33 = analogRead(detPin3);
      float detSensor43 = analogRead(detPin4);

      float detSensor14 = analogRead(detPin1);
      float detSensor24 = analogRead(detPin2);
      float detSensor34 = analogRead(detPin3);
      float detSensor44 = analogRead(detPin4);

      float detSensor15 = analogRead(detPin1);
      float detSensor25 = analogRead(detPin2);
      float detSensor35 = analogRead(detPin3);
      float detSensor45 = analogRead(detPin4);
```

```
      float detSensor1 =
(detSensor11+detSensor12+detSensor13+detSensor14+detSensor15)/5;
      float detSensor2 =
(detSensor21+detSensor22+detSensor23+detSensor24+detSensor25)/5;
      float detSensor3 =
(detSensor31+detSensor32+detSensor33+detSensor34+detSensor35)/5;
      float detSensor4 =
(detSensor41+detSensor42+detSensor43+detSensor44+detSensor45)/5;
      //Add the new data to an output string
      dataStr += String(tempSensor);
      dataStr += ",";
      dataStr += String(detSensor1);
      dataStr += ",";
      dataStr += String(detSensor2);
      dataStr += ",";
      dataStr += String(detSensor3);
      dataStr += ",";
      dataStr += String(detSensor4);
      dataStr += ",";
      dataStr += String(millis());
      dataStr += "/n";

      //Reset the circuit
      digitalWrite(outputPin, HIGH);
      delay(10);
      digitalWrite(outputPin, LOW);
      //Update time
      t = millis();
    }
  }
  //Open the output file
  File dataFile = SD.open("datalog.txt", FILE_WRITE);
  //Write to output file
  if (dataFile) {
    dataFile.println(dataStr);
    dataFile.close();
    //Also print the data to the serial port
    Serial.println(dataStr);
  }
  else {
    Serial.println("Error in opening output file!");
  }
}
```

**Appendix B: References**


[1] G. F. Knoll, *Radiation Detection and Measurement*: John Wiley & Sons, Inc., 2000.

[2] E. Technologies. (2018). *General Purpose, EJ-200*. Available: https://eljentechnology.com/products/plastic-scintillators/ej-200-ej-204-ej-208-ej-212

[3] D. J. Wagenaar. (2018). *Charged Particle Range*. Available: http://www.med.harvard.edu/jpnm/physics/nmltd/radprin/sect7/7.2/7_2.1.html

[4] P. O. Lab. (2018). *Backscattering of Beta Particles*. Available: http://physicsopenlab.org/2017/02/27/backscattering-of-beta-particles/

[5] K. J. Shultis, *Radiaiton Shielding*: American Nuclear Society, 2000.

[6] T. H. Kim. (2008). *Compton Scattering*. Available: https://web.stanford.edu/~kimth/www-mit/8.13/Compton/_paper/thk_compton.pdf

[7] *Analytical Instruments*. Available: http://analyticalprofessional.blogspot.com/2013/05/photomultiplier-tube.html

[8] SensL, "C-Series SiPM."

[9] SensL. (2017). *An Introduction to Silicon Photomultiplier Technology*. Available: https://www.sensl.com/downloads/ds/TN%20-%20Intro%20to%20SPM%20Tech.pdf

[10] *Wikimedia Commons*. Available: https://commons.wikimedia.org/wiki/File:Sallen-Key_Generic_Circuit.svg

[11] "Patent #4968898."

[12] *Planet Analog*. Available: https://www.planetanalog.com/author.asp?section_id=396&doc_id=562072

[13] *Circuits Today*. Available: http://www.circuitstoday.com/sample-and-hold-circuit